Journal of Power Sources 195 (2010) 11–20

Contents lists available at ScienceDirect

Journal of Power Sources

journal homepage: www.elsevier.com/locate/jpowsour

Preparation of sulfonated poly(ether ether ketone)s containing amino groups/epoxy resin composite membranes and their in situ crosslinking for application in fuel cells

Meimei Guo, Baijun Liu, Long Li, Chang Liu, Lifeng Wang, Zhenhua Jiang*

Alan G. MacDiarmid Institute, Jilin University, 2699 Qianjin Street, Changchun 130012, PR China

ARTICLE INFO

Article history:
Received 22 May 2009
Received in revised form 12 July 2009
Accepted 13 July 2009
Available online 21 July 2009

Keywords:
Composite membranes
Reaction kinetics
Methanol permeability
Fuel cells

ABSTRACT

A series of amino-containing sulfonated poly(aryl ether ketone)/4,4′-diglycidyl(biphenyl) epoxy resin (DGBP) composite membranes for proton exchange membranes fuel cells (PEMFCs) are prepared by solution blending and casting. The reaction kinetics and the effects of introduction of DGBP content on the properties of the composite membranes are thoroughly investigated. The crosslinked composite membranes after treatment at either 120 °C or 200 °C have improved oxidative and dimensional stability than those without crosslinking. Despite the fact that crosslinked membranes generally have lower proton conductivity in comparison with the original ones, the proton conductivities of the membranes treated at 120 °C are above 2.22×10^{-2} S cm^{-1} at room temperature and 9.42×10^{-2} S cm^{-1} at 100 °C. Even for the samples treated at 200 °C, their proton conductivities are still higher than 1.26×10^{-2} S cm^{-1} at room temperature and higher than 8.67×10^{-2} S cm^{-1} at 100 °C, which are well satisfied with elementary requirement of fuel cells. In addition, all the evaluated membranes have low methanol permeability. For example, the methanol permeability of AP6FSPEEK/DGBP1 cured at 200 °C is 0.33×10^{-6} cm^2 s^{-1}, which is an order magnitude lower than Nafion 117. Therefore, these novel crosslinked composite membranes could be potential usage in fuel cells.

1. Introduction

The search for renewable, clean energy sources is one of the most pressing challenges facing global society. Known as their high efficiency, simply design, low emissions and low operating temperatures, proton exchange membrane fuel cells (PEMFCs) and direct methanol fuel cells (DMFCs) are receiving considerable attention as electric power sources for automobile or portable devices [1]. Perfluorosulfonic acid PEMs, such as Dupont's Nafion, are typically used as the polymer electrolytes in PEMFCs due to their excellent chemical and mechanical stabilities as well as high proton conductivity. However, high cost, low operation temperature (≤80 °C), high methanol crossover, and environmental recycling uncertainties of Nafion and other similar perfluorinated membranes are limiting their widespread commercial application in PEMFCs and DMFCs [1–4]. For this reason, many researchers hope to develop high performance, low cost and high proton conductive electrolyte membranes. Aromatic polymers with sulfonic acid groups are promising alternative materials for PEMFCs. Among the alternative materials investigated, sulfonated poly(arylene ether ketone)s [4], sulfonated poly(arylene ether sulfone)s [5–7], sulfonated polyimides [8], sulfonated poly(arylene ether nitrile)s [9], and sulfonated poly(benzimidazole)s [10] have been studied due to their high thermal and chemical stability, high proton conductivity and low cost.

Because of their excellent mechanical strength, and thermooxidative and chemical resistance [11], sulfonated poly(aryl ether ketone)s (SPAEKs), as one of alternative PEM materials [12], have aroused researchers' interests [13]. It is found that SPAEKs with high ion-exchange capacities often have relatively high swelling ratio and low mechanical strength under humid circumstance at high temperature [12,13], which limits their application for PEMFCs. To solve these problems, several approaches have been adopted and some results are interesting. McGrath's group has studied the influence of microstructure/sequence distribution on the performance properties of proton exchange membranes [14], and they found that the ideal phase separated morphology of the membranes based on the multiblock polymers enhanced proton conductivity under partially hydrated conditions. However, the synthesis routes are complicated and high molecular weight polymers could not be easy to obtain. Liu et al. [15] and Lee et al. [16] recently reported different kinds of PEMs crosslinked by an esterification reaction between –COOH and –OH, respectively. They found that the crosslinking reaction could play an important role in dimensional stability.

* Corresponding author. Tel.: +86 431 85168886; fax: +86 431 85168868.
E-mail address: jiangzhenhua@jlu.edu.cn (Z. Jiang).

0378-7753/$ – see front matter © 2009 Elsevier B.V. All rights reserved.
doi:10.1016/j.jpowsour.2009.07.025

Unfortunately, the introduction of poly(vinyl alcohol) (PVA) with aliphatic main chain might destroy the thermal stability. Na and co-workers has investigated UV crosslinking membranes [17], and found that this method could effectively improve the properties of PEMs. However, ultraviolet radiation could not penetrate the membranes and the crosslinking reaction mainly occurred on the surface of membranes, which led to poor homogeneous properties of membranes.

Epoxy resins have been widely used as high performance materials in many fields, such as adhesive, coating, laminating capsulation, electrical insulation and composite applications [18–20]. The epoxy resins have exhibited good thermal properties, chemical resistance and electric insulation through a crosslinking reaction with a curing agent to form a three-dimensional network structure. Recently, epoxy resins containing bulky moiteies such as dicyclopentadiene, biphenyl, naphthalene, fluorene, maleimide or silsesquioxane moieties have been synthesized as new families of high performance polymers [21–24]. Among them, rigid rod epoxy resins with good thermal stability and unique physical properties have been developed as high performance polymers for electronic and aerospace applications, and in particular potentially enhanced thermal stability and dielectric properties over conventional epoxy resins [25–27]. It may be an efficient way to obtain the PEMs having an excellent combination of high proton conductivity, good thermal-oxidative and dimensional stability through the incorporation of epoxy resins into the sulfonated polymer matrix. Most recently, Na and co-workers has prepared epoxy solidified membranes [28]. It is obvious that epoxy crosslinking could occur and avoid the above mentioned shortcomings of UV-irradiation crosslinking [17]. However, a third component of amine as curing agent has to be introduced into this composite system, and it makes the preparing and curing process of membrane more complex.

In a previous work [29], we have prepared a series of molecule-enhanced blend membranes comprising of an aminated polymer and sulfonated polymers, and their properties were more excellent than a copolymer bearing both amino groups and sulfonic acid groups (AP6FSPEEK). Although the introduction of amino group by direct polymerization could be effective in decreasing water uptake and swelling ratio by acid–base interaction, the interaction could be weakened in high temperature. In this work, as a continuous study, we prepare a new family of composite membranes based on a kind of epoxy resin with rigid rod biphenyl structure (DGBP) and copolymer with double functional groups (AP6FSPEEK). Direct in situ polymerization between DGBP and AP6FSPEEK occurs when the composites are treated at given temperature. The reaction kinetics and the effects of introduction of DGBP into AP6FSPEEK on the water uptake, swelling ratio, thermal stability and proton conductivity are investigated thoroughly.

2. Experimental

2.1. Materials

(4-Amino)phenylhydroquinone (4-AmPHQ) was synthesized in our lab through a two-step coupling–reduction reaction [29,30]. 4,4′-Difluorobenzophenone (DFBP) was purchased from Yianbian Chemical Factory (China) and purified by recrystallization from a mixture of ethanol and deionized water. Sodium 5,5′-carbonylbis(2-fluorobenzene-sulfonate) (SDFBP) was prepared according to the procedure described by Wang et al. [31]. K_2CO_3 (Beijing Chemical Reagent, China) was ground into fine powder and dried at 120 °C for 24 h before polymerization. 4,4′-(Hexafluoroisopropylidene)diphenol (6FBPA, Aldrich), 4,4′-biphenol (BP, Honsyu Chemical Co. Ltd., Japan), epichlorohydrin (Tianjin Huadong Chemical Factory, China), sodium hydroxide (Tianjin Reagent Plant, China), and Tetrabutyl ammonium hydrogen sulfate (TBAHS, Shanghai Hero Chem Chemical Co. Ltd., China) were used as received. All the other organic solvents were obtained from commercial sources and purified by conventional methods.

2.2. Synthesis of AP6FSPEEK and DGBP

The amino-containing sulfonated copolymer (AP6FSPEEK) was synthesized using the same procedure as our previous work [29]. 4,4′-Diglycidyl(biphenyl) epoxy resin (DGBP) was synthesized according to the reported procedures [32–34].

AP6FSPEEK: ^{1}H NMR (DMSO-d_6, δ, ppm): 8.25 (m, 2H), 7.83 (d, 4H), 7.74 (d, 2H), 7.44–7.39 (m, 7.2H), 7.24–7.15 (m, 11.8H), 7.07 (d, 2H), 7.01–6.53 (m, 0.8H), 5.31 (s, 0.4H).

DGBP: ^{1}H NMR (DMSO-d_6, δ, ppm): 7.55 (d, 4H), 7.03 (d, 4H), 4.33–4.38 (dd, J = 11.4 Hz, J = 2.6 Hz, 2H), 3.83–3.89 (dd, J = 11.4 Hz, J = 6.6 Hz, 2H), 3.32–3.37(m, 2H), 2.84–2.87 (t, J = 4.3 Hz, 2H), 2.71–2.74 (dd, J = 5.1 Hz, J = 2.6 Hz, 2H).

Melting point: 155–163 °C (DSC); m/z: 298.

FT-IR (KBr, cm^{-1}): 2930 (–CH_2O–), 1242 and 1027 (C–O–C), 911 (oxirane).

2.3. Preparation of composite membranes

AP6FSPEEK membrane and the AP6FSPEEK/DGBP composite membranes were prepared by solution casting and evaporation method. The pure membrane named as AP6FSPEEK was cast from 10% (w/v) solution directly. However, for the composite membranes, more processes were needed. First, the AP6FSPEEK was dissolved in DMAc at room temperature to prepare a 10% (w/v) solution. Secondly, equivalent DGBP was added into the homogeneous solution, and the composite membrane was obtained by solution casting after stirring for 24 h. At last, the membrane named as AP6FSPEEK/DGBP1 was transformed to its acid form by ion exchange in 0.5 M H_2SO_4 for 2 h at 80 °C, and then washed with deionized water until the pH reached 6–7. As comparison, we prepared two more composite membranes with 1.5 equivalent and 2.0 equivalent DGBP, and they were named as AP6FSPEEK/DGBP1.5 and AP6FSPEEK/DGBP2, respectively. All the membranes were divided into two parts, and cured at different temperature. One part was treated at 200 °C for 0.5 h for enhancing thermal activation of the crosslinking reaction between DGBP and AP6FSPEEK, and then at 120 °C for 24 h. The other was heated at 120 °C for 24 h. The thickness of membranes was in the range of 40–65 μm.

2.4. Characterization

^{1}H NMR experiments were carried out on a Bruker 510 spectrometer (500 MHz) using DMSO-d_6 as solvent. MALDI-TOF mass spectra were obtained on a Kratos of Shimadzu Company. FT-IR spectra were recorded via the KBr pellet method by using a Nicolet Impact 410 FT-IR spectrophotometer. Differential scanning calorimeter (DSC) measurements were performed on a Mettler Toledo DSC821^e instrument from 50 to 400 °C at heating rates of 5, 10, 15 and 20 °C min^{-1} under nitrogen atmosphere at a constant flow of 200 mL min^{-1}. Thermogravimetric analysis (TGA) was employed to assess thermal stability of membranes with a Netzch Sta 449c thermal analyzer system. Before analysis, the films were dried and kept in the TGA furnace at 150 °C for 15 min. The samples were cooled to 80 °C and then reheated to 800 °C in nitrogen and 700 °C in air at 10 °C min^{-1}. The temperatures at 5% and 10% weight loss were recorded for each sample.

2.5. Curing kinetics of composite membranes

Curing is the essential process for the application of hardening epoxy resins. The study of the curing kinetics could be used to optimize the curing conditions. DSC has been extensively used to characterize the curing kinetics of thermoset resins in dynamic or isothermal modes [35–37]. In this study, we use the nonisothermal DSC method to study the thermal curing behaviors of AP6FSPEEK/DGBP systems at heating rates of 5, 10, 15 and 20 °C min^{-1}.

Many equations are developed to investigate the curing kinetics of the epoxy system. Kissinger and Ozawa methods [38,39] are two common methods that are applied to calculate activation energy (E) and frequency factor (A). Both of them are reported in their previous articles [33,34].

Kissinger's equation can be expressed as follows:

$$-\ln\frac{\beta}{T_p^2} = \frac{E_k}{RT_p} - \ln\frac{AR}{E_k} \tag{1}$$

where A, R are Arrenihus constant and ideal gas constant, respectively. T_p, β are peak temperature of cure exotherms and DSC heating rates, respectively. E_k is activation energy calculated from Kissinger's equation. Therefore, E_k could be obtained from the slope of $\ln(\beta/T_p^2)$ vs. $1/T_p$ plot.

Ozawa's equation is:

$$E_o = -\frac{R}{1.052} \times \frac{d\ \ln\beta}{d(1/T_p)} \tag{2}$$

where R is ideal gas constant. T_p, β are peak temperature of cure exotherms and DSC heating rates, respectively. E_o is activation energy calculated from Ozawa's equation. E_o could be obtained from the slope of $\ln(\beta)$ vs. $1/T_p$ plot.

According to Kissinger's equation, A can be calculated with the following equation. Where E_a is activation energy:

$$A = \frac{\beta E_a \exp[E_a/RT_p]}{RT_p^2} \tag{3}$$

Furthermore, the curing reaction order (n) could be obtained [40] in the following:

$$\frac{d(\ln\ \beta)}{d(1/T_p)} = -\left[\frac{E_{a,k}}{nR} + 2T_p\right] \tag{4}$$

where $E_{a,k}$ is activation energy calculated by Kissinger's method.

2.6. Oxidative and hydrolytic stability

A small piece of the membrane sample is soaked in Fenton's reagent (3% H_2O_2 containing 2 ppm $FeSO_4$) at 80 °C. The oxidative stability is evaluated by recording the time when the membranes disappeared and the retained weights of membranes after treating in Fenton's reagent for 1 h at 80 °C.

2.7. Methanol permeability

The methanol diffusion coefficient is determined using a cell basically consisting of two-half-cells separated by the membrane, which is fixed between two rubber rings. Methanol solutions (10 mol L^{-1}) are placed on one side of the cell and pure water is placed on the other side. The magnetic stirrers are used continuously during the measurement. Methanol concentrations in the water cell are periodically determined by using a GC-14C gas chromatograph (SHTMADU, Tokyo, Japan). Peak areas are converted into methanol concentration with a calibration curve. The methanol diffusion coefficient is calculated according to the following equation:

$$C_B(t) = \frac{A}{V_B}\frac{DK}{L}C_A(t - t_0) \tag{5}$$

2.8. Water uptake and swelling ratio measurements

The water uptake of the membranes at different temperatures is calculated by measuring the weight difference between the dry and wet swollen membranes as follows [29,41,42]: the sample films (1 cm × 4 cm) are all dried at 120 °C for 24 h prior to the measurements. After measuring the lengths and weights of dry membranes, the sample films are soaked in deionized water to reach equilibrium at desired temperature. Before measuring the lengths and weights of hydrated membranes, the water is removed from the membrane surface by blotting with a paper towel. The water uptake is calculated by the following equation:

$$\text{Water uptake}\,(\%) = \frac{W_{wet} - W_{dry}}{W_{dry}} \times 100\% \tag{6}$$

where W_{dry} and W_{wet} are the weights of dried and wet samples, respectively.

Dimensional change of the copolymer membranes is investigated by immersing the sample films (1 cm × 4 cm) in deionized water to reach equilibrium at desired temperature. The change of film length is calculated from:

$$\text{Swelling ratio}\,(\%) = \frac{L_{wet} - L_{dry}}{L_{dry}} \times 100\% \tag{7}$$

where L_{wet} and L_{dry} are the lengths of the wet and dry membranes, respectively.

2.9. Proton conductivity

Proton conductivity measurements are conducted on a Solatron-1260/1287 impedance analyzer over a frequency range of 10–10^6 Hz with 50–500 mV oscillating voltage. A sheet of the sulfonated membrane (30 mm × 10 mm) is placed in a test cell [41]. Before the measurements, the membranes are fully hydrated in water at different temperatures for 48 h. Conductivity measurements of fully hydrated membranes are carried out with the cell immersed in liquid water at the desired temperature. The conductivity (σ) of the membranes in the transverse direction is calculated from the following equation:

$$\sigma = \frac{D}{RA} \tag{8}$$

where D is the distance between the two electrodes. R and A are the measured resistance and transverse area of the film samples, respectively.

3. Results and discussion

3.1. Synthesis of AP6FSPEEK and DGBP

To make PEMs with acceptable dimensional change under hot and humid circumstance, fluorine-containing monomer, 6FBPA, is selected to prepare sulfonated poly(ether ether ketone) by direct copolymerization [13]. However, the swelling ratio is still too high when their sulfonated degrees are high. Thus, we need another method to achieve the goal of low swelling. In our previous work, we have studied the acid–basic interaction in PEMs, and found that the introduction of amino group by copolymerization could decrease the swelling ratio and water uptake to some extent [29]. However, the decrease of the swelling was limited and the excess swelling was still existed at high temperature due to the weak acid–basic interaction. Since covalent bond is less sensitive

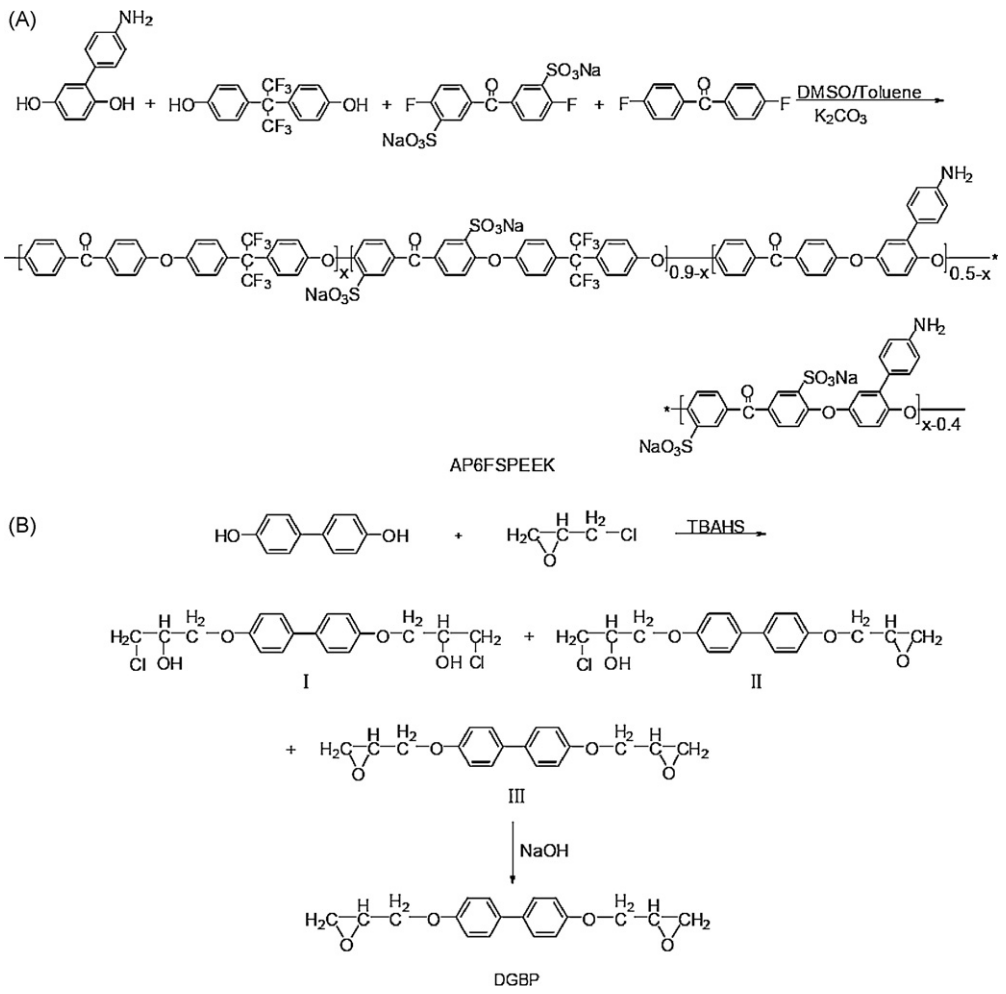

Scheme 1. Preparation route and chemical structure of AP6FSPEEK (A) and DGBP (B).

to temperature than acid–basic interaction, an epoxy solidified crosslinking method is selected in this study. A kind of biphenyl containing rod epoxy resin (DGBP) having good thermal stability and good solubility is synthesized. Generally, the small-molecular amines have to be used as a catalyst for the crosslinking reaction of epoxy resin [27,33]. In order to avoid the incorporation of the small-molecular compound or a third amine catalyst into the system, AP6FSPEEK containing both amino groups and sulfonic acid groups is selected. The amino groups on the backbones of polymers are expected to serve as catalyst. The synthesis routes of AP6FSPEEK and DGBP are shown in Scheme 1. The characterization of AP6FSPEEK is given in our previous work [29], and FT-IR, ^{1}H NMR are used to character the structure of DGBP (the data are shown in Section 2.2). Due to the good solubility of DGBP and AP6FSPEEKK in N,N-Dimethylacetamide (DMAc), the uniform thin membranes could be made by the solution cast from their solutions in DMAc. Crosslinked composite membranes are prepared by thermal activation according to the process of Section 2.3. The FT-IR spectra are usually used to confirm the structure. The curves of AP6SPEEK/DGBP1 cured at 120 °C (a), 200 °C (b) and epoxy resin (c) are shown in Fig. 1. The characteristic peak at 911 cm^{-1} is assigned to stretching vibration of oxirane, and disappears in the cured composite membranes of AP6SPEEK/DGBP1. The results illuminate that the oxirane reacts in the process of heat curing. The characteristic peaks at 1242–1272 cm^{-1} assigned to stretching vibration of C–O–C and the peaks around 520 cm^{-1} assigned to bending vibration of C–O–C appear in the three curves, because the ether bonds exist before and after crosslinking. However, another C–O–C peak at 1027 cm^{-1} is not observed at the same wavenumber in Fig. 1(a) and (b), the probable reason is that the characteristic peaks of sulfonic groups at 1025 cm^{-1} overlaps with the peak of C–O–C.

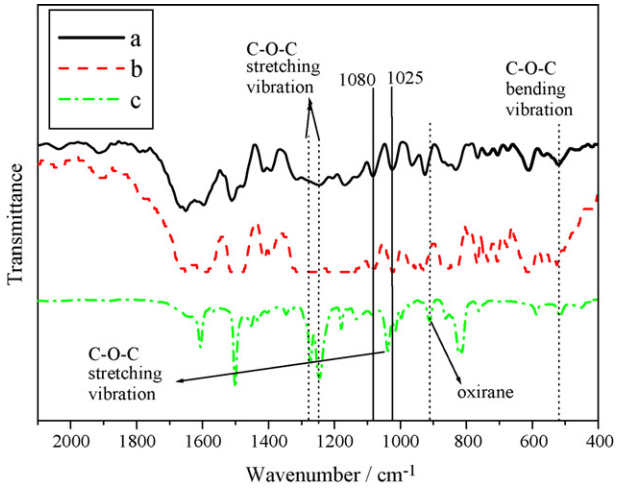

Fig. 1. FT-IR spectra of AP6SPEEK/DGBP1 cured at 120 °C (a), 200 °C (b) and epoxy resin (c).

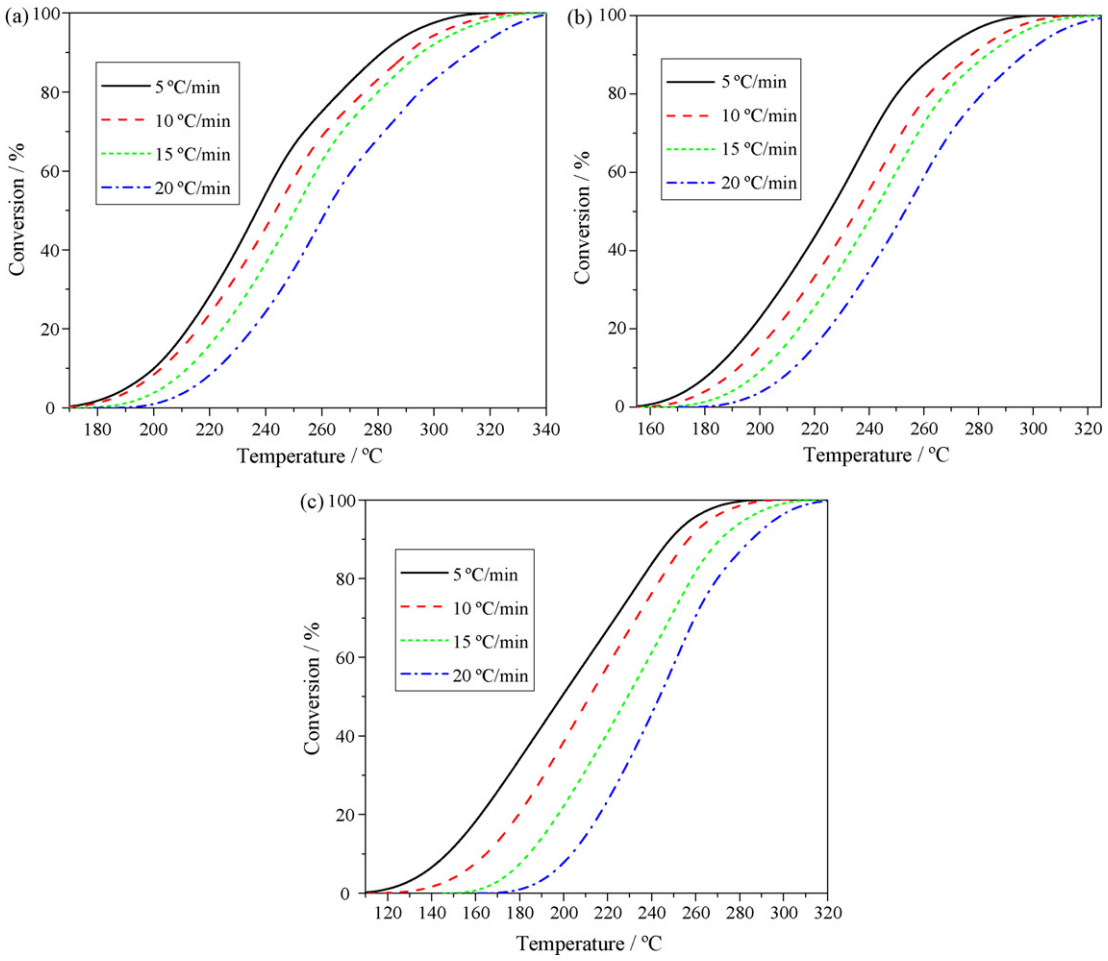

Fig. 2. Fractional conversions as a function of temperature for various heating rates for the composite membranes (a) AP6FSPEEK/DGBP1, (b) AP6FSPEEK/DGBP1.5 and (c) AP6FSPEEK/DGBP2.

3.2. Curing kinetics of AP6FSPEEK/DGBP systems

The exothermic peak temperatures (T_ps) of the curing process, which are summarized in Table 1, shift to higher temperature with increasing heating rate (β) of each composite membrane. The T_ps decrease with increasing the content of DGBP in composite membranes at each heating rate. Fig. 2 shows the fractional conversions as a function of temperature at various heating rates for the AP6FSPEEK/DGBP system. It could be seen that the isoconversional temperature increases with increasing the heating rate for the systems in each figure, and the initiative crosslinking temperature decreases with increasing the content of DGBP. It is accordant to the trend of E of composite materials (Table 2). The isoconversional plots by Kissinger and Ozawa mode are given in Figs. 3 and 4, respectively.

On the basis of the experimental results from the dynamic DSC study, E, A and n of the AP6FSPEEK/DGBP systems are obtained using Eqs. (1)–(4). As shown in Table 2, the values of activation energy are not a constant, and the values of E_k and E_o are 28.92–31.43 kJ mol^{-1} and 31.43–32.91 kJ mol^{-1}, respectively. We find the values of E_k and E_o decrease with increasing the content of DGBP. This might be attributed to the existence of more reactive points with increasing the content of DGBP in membranes, and it makes the crosslinking reaction easier. Thus, crosslinking

Table 1
Peak temperature (T_p, °C) of cure exotherms for the AP6FSPEEK/DGBP system at different DSC heating rates (β).

Samples	β (°C min^{-1})			
	5	10	15	20
AP6FSPEEK/DGBP1	237	247	252	258
AP6FSPEEK/DGBP1.5	236	246	251	257
AP6FSPEEK/DGBP2	232	245	248	252

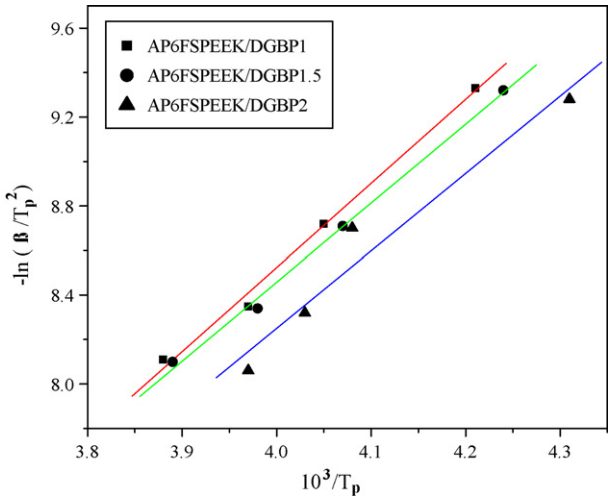

Fig. 3. Plot for determination of the E and the A by Kissinger method in curing reactions.

Table 2
Curing kinetic parameters for the AP6FSPEEK/DGBP system derived from the multi-temperature scan method.

Samples	Kissinger method			Ozawa method	
	E_k (kJ mol^{-1})	A (s^{-1})	n	E_o (kJ mol^{-1})	A (s^{-1})
AP6FSPEEK/DGBP1	31.43	2.785×10^6	0.970	32.91	5.974×10^6
AP6FSPEEK/DGBP1.5	29.52	1.107×10^6	0.996	31.86	3.733×10^6
AP6FSPEEK/DGBP2	28.92	1.059×10^6	1.003	31.43	3.636×10^6

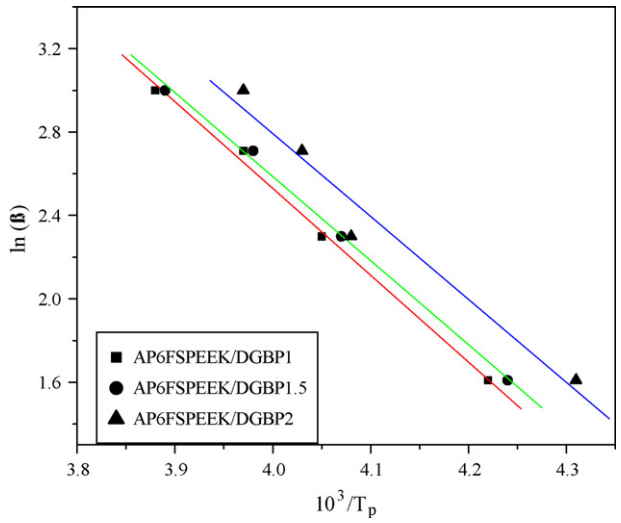

Fig. 4. Plot for determination of the E and the A by Ozawa method in curing reactions.

reaction could occur at lower temperature (Fig. 2). Although the initial temperatures (T_is) decrease to about 120 °C with increasing the content of DGBP, the peak temperatures (T_ps) are high. Considering the degradation of sulfonic groups at high temperature and the data of curing kinetics of composite membranes systems, we select two procedures described in Section 2.3 to cure the composite membranes, and research the effect of different curing temperature. The schematic illustration and the possible chemical reaction mechanism of the curing process are shown in Schemes 2 and 3, respectively.

3.3. Oxidative stability and thermal properties of composite membranes

Oxidative stability of curing membranes is examined by observing their dissolving behaviors in Fenton's Reagent at 80 °C. This method is regarded as one of the standard tests to gauge relative oxidative stability and to simulate accelerated fuel cell operating conditions [13]. All the membranes exhibit excellent oxidative stability, as shown in Table 3. For the crosslinked membranes, 99% weight is retained after treating in Fenton's reagent at 80 °C for 1 h, and they all do not dissolve in Fenton's reagent within 4 h. These results are much better than that of AP6FSPEEK. Moreover, the composite membranes cured at 200 °C show more excellent oxidative stability and they do not dissolve in the reagent within 6 h. This might be because that the crosslinking reaction of DGBP is more complete after high temperature curing (Scheme 2), and the crosslinking network structure improves the oxidative stability of composite membranes.

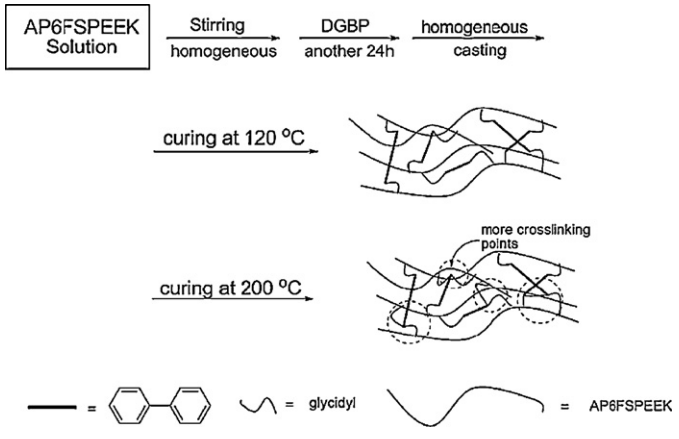

Scheme 2. Schematic illustration for the preparation of composite membranes.

The thermal properties are one of the important factors on the usage of PEMs. Thermal stabilities of AP6FSPEEK/DGBP composite membranes in acid forms after curing are investigated by TGA in nitrogen and air. All of the membranes exhibit two distinct degradation steps. The first step in pure membrane is associated with the loss of degradation of the sulfonic acid groups, and the second is related with the degradation of the polymer's backbones. However, in the composite membranes, the first step might be associated with the loss of the sulfonic acid groups and the partial degradation of DGBP, and the second step is associated with main chain of crosslinked polymers. Being similar to other report [28], although the decomposition temperatures of composite membranes are lower than pure membrane, as shown in Fig. 5(c) and (a), they still well meet the requirement of PEMFCs about operating temperature. Comparing Fig. 5(c) with Fig. 5(b), we can see that composite membrane cured at high temperature has better thermal stability. Because fuel cell operates in redox conditions, we also test the thermal stability of membranes in air condition (Fig. 6). Although the decomposition in air is a little faster than that in nitrogen, the decomposition temperatures of T_{onset}, $T_{d5\%}$ and $T_{d10\%}$ in air are close to that in nitrogen (Table 4). Data of decomposition temperatures in both nitrogen and air are summarized in Table 4. Although the decomposition temperatures decrease with increasing DGBP content, the onset decomposition temperatures (T_{onset}) of all the crosslinked samples are all above 261 °C in nitrogen and above 282 °C in air. Especially after curing at 200 °C, the T_{onset} is obviously improved for composite membranes, which might be attributed to the formation of more crosslinking network structure cured at 200 °C (Scheme 2). This result indicates that these membranes have good thermal stability.

Table 3
Oxidative stability of membranes.

Polymer	Oxidative stability			
	RW (%)[a]	RW (%)[b]	t (h)[c]	t (h)[d]
AP6FSPEEK	~97	~97	4 h	4 h
AP6FSPEEK/DGBP1	~99	~99	~4.5 h	>6 h
AP6FSPEEK/DGBP1.5	~99	~99	~4.5 h	>6 h
AP6FSPEEK/DGBP2	~99	~99	5 h	>6 h

[a,b] Retained weights of membranes cured at 120 °C and 200 °C after treating in Fenton's reagent for 1 h at 80 °C, respectively.
[c,d] The dissolved time of polymer membranes cured at 120 °C and 200 °C in Fenton's reagent at 80 °C, respectively.

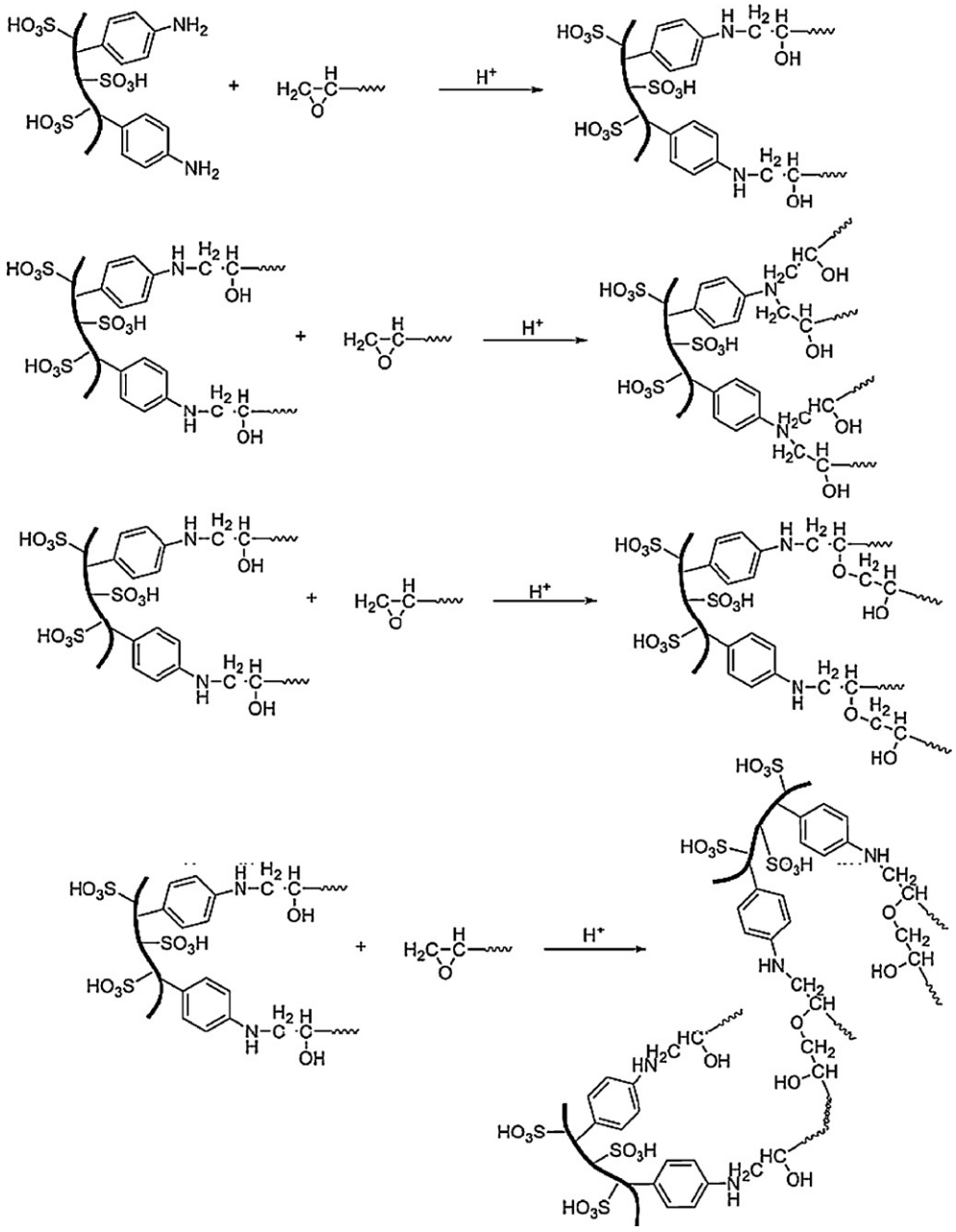

Scheme 3. Chemical reaction mechanism between DGBP and AP6FSPEEK.

3.4. Ionic exchange capacity and methanol permeability of membranes

Before curing, the composite membranes all show good solubility in high polar aprotic solvents. Although the membranes without DGBP cured at 120 °C and 200 °C still have good solubility in common solvents, the composite membranes treated at the same conditions could not be dissolved even at heating. It exhibits that the crosslinking reaction occurred in composite membranes at both 120 °C and 200 °C. And it plays an important

Table 4
Thermal properties of membranes.

Polymer	$T_{d(5\%)}$ (°C)			$T_{d(10\%)}$ (°C)			T_{onset} (°C)		
	T_{d1} [a]	T_{d2} [b]	T_{d3} [c]	T_{d1} [a]	T_{d2} [b]	T_{d3} [c]	T_1 [a]	T_2 [b]	T_3 [c]
AP6FSPEEK	344	351	352	372	388	383	311	317	329
AP6FSPEEK/DGBP1	298	323	330	347	372	374	265	284	302
AP6FSPEEK/DGBP1.5	295	312	321	329	358	372	263	277	284
AP6FSPEEK/DGBP2	294	308	317	328	349	370	261	270	282

[a] Data in nitrogen cured at 120 °C.
[b] Data in nitrogen cured at 200 °C.
[c] Data in air cured at 200 °C.

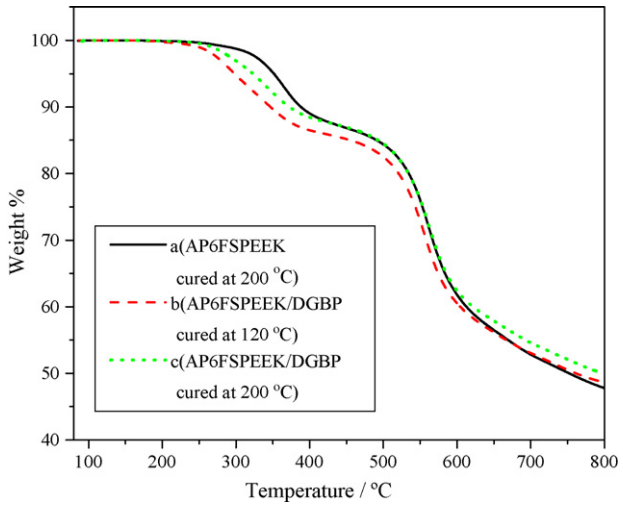

Fig. 5. TGA curves of the samples. (a) AP6FSPEEK cured at 200 °C, (b) AP6FSPEEK/DGBP1 cured at 120 °C and (c) AP6FSPEEK/DGBP1 cured at 200 °C.

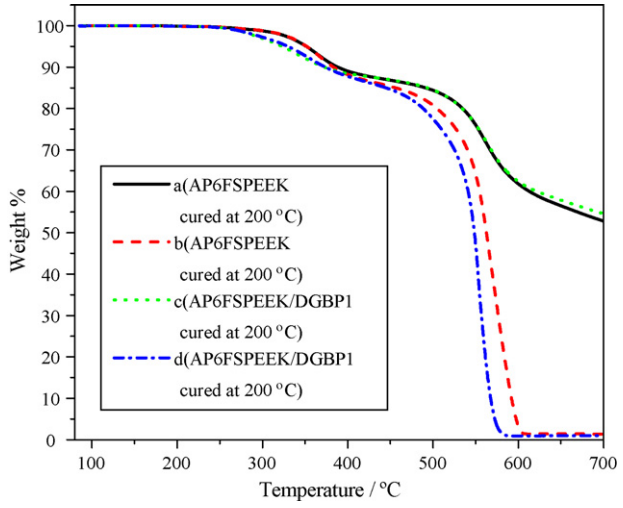

Fig. 6. TGA curves for AP6FSPEEK and AP6FSPEEK/DGBP1 cured at 200 °C in nitrogen (a and c) and in air (b and d).

role for PEM with high ion exchange capacity (IEC) in alcohol resistance property [28]. After acidification and curing, the ion exchange capacity (IEC) values of these acid-form membranes are determined by classical acid–base titration [42,43]. As shown in Table 5, the experimental IEC values of the samples treated at

Table 5
IEC values and methanol permeability.

Polymer	IEC			Methanol permeability ($\times 10^{-6}$ cm^2 s^{-1})	
	A[a]	B[b]	C[c]	120 °C[d]	200 °C[e]
AP6FSPEEK	1.72	1.65	1.61	0.47	0.37
AP6FSPEEK/DGBP1	1.64	1.33	1.26	1.28	0.33
AP6FSPEEK/DGBP1.5	1.56	1.28	1.18	1.76	0.85
AP6FSPEEK/DGBP2	1.49	1.12	1.12	2.01	1.11
Nafion 117[f]	–	–	–	2.94	

[a] Theoretical value (mmol g^{-1}).
[b] Experimental value of membrane cured at 120 °C (mmol g^{-1}).
[c] Experimental value of membrane cured at 200 °C (mmol g^{-1}).
[d] Membranes cured at 120 °C.
[e] Membranes cured at 200 °C.
[f] Data measured in our laboratories with the same condition as composite membranes.

Table 6
Water uptake of membranes at different temperature.

Polymer	Temperature (°C)					
	20		80		100	
	WU_1[a]	WU_2[b]	WU_1[a]	WU_2[b]	WU_1[a]	WU_2[b]
AP6FSPEEK	20.2	11.6	36.5	32.8	69.3	43.6
AP6FSPEEK/DGBP1	18.1	9.8	32.1	27.0	59.2	36.8
AP6FSPEEK/DGBP1.5	13.3	6.5	30.4	25.8	54.1	33.8
AP6FSPEEK/DGBP2	10.1	5.6	21.9	18.1	33.7	29.0

[a] Water uptake (%) of membranes cured at 120 °C.
[b] Water uptake (%) of membranes cured at 200 °C.

120 °C and 200 °C are in the range of 1.12–1.65 and 1.12–1.61, respectively.

Methanol permeability is one of the important transport properties, which determines the fuel cell performance in direct methanol fell cells (DMFCs) [28,41]. In DMFC, the PEM is required to have low methanol diffusion coefficient because the diffusion of methanol from the anode to the cathode lead to power loss and other undesirable consequences. The membranes with lower methanol diffusion coefficient may allow for higher methanol feed concentration, thereby increasing the effective energy density of the fuel cell system. As shown in Table 5, there is an interesting phenomenon. The methanol permeability increases when the content of DGBP increases in the composite membrane in both heat treatment condition, respectively. It may be caused by the introduction of the aliphatic moieties, which leads to the increase of methanol permeability. Methanol permeability of each membrane cured at 200 °C is lower than that cured at 120 °C. For pure membrane, it might attribute to the effective alcohol resistance of compact microstructure with high temperature treatment. For composite membranes, the more crosslinked compact structure, which is competitive effect with aliphatic chain in methanol permeability, makes less methanol permeability. Comparing the crosslinking effect with aliphatic chain effect, the membrane of AP6FSPEEK/DGBP1 cured at 200 °C shows the excellent alcohol resistance. However, the methanol permeability of pure and composite membranes is all still lower than commercial Nafion 117 and the methanol permeability of most of the membranes cured at 200 °C is an order magnitude lower than Nafion 117. Particularly, the membrane of AP6FSPEEK/DGBP1 cured at 200 °C could reach the minimum of 0.33×10^{-6} cm^2 s^{-1}, and it might be promising candidate for DMFCs.

3.5. Water uptake and swelling ratio of membranes

For most proton conductive polymers, water plays an important role in the proton exchange membrane and acts as the carrier for proton transportation through the polymer membrane [44,45]. Adequate hydration of electrolyte membranes is crucial for high proton conductivity. However, excess water uptake in electrolyte membranes results in unacceptable dimensional change or loss of dimensional shape, which could lead to weakness or a dimensional mismatch when incorporated into a membrane electrode assembly (MEA) [13]. Thus, proper water uptake is needed for dimensional stability and application for PEMs. The water uptake and swelling ratio of the membranes cured at different temperature are measured. The curves of water uptake and swelling ratio vs. the content of DGBP are shown in Figs. 7 and 8. The shapes of the water uptake curves for membranes are found to be similar. For each membrane, the water uptake decreases with increasing the content of DGBP at the same temperature, while it increases with increasing temperature. The data of water uptake and swelling ratio are tabulated in Tables 6 and 7, repetitively. From these data, we can see that the water uptake and swelling ratio decrease obviously cured at both 120 °C and 200 °C. Particularly, after curing at 200 °C, the values of

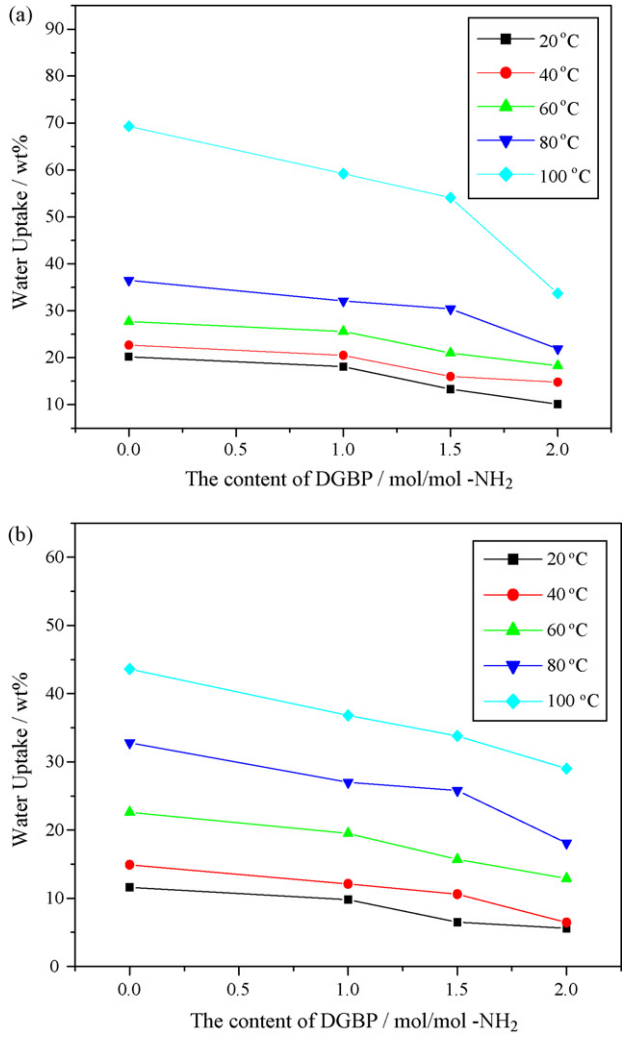

Fig. 7. Water uptake of membranes cured at 120 °C (a) and 200 °C (b) with different content of DGBP.

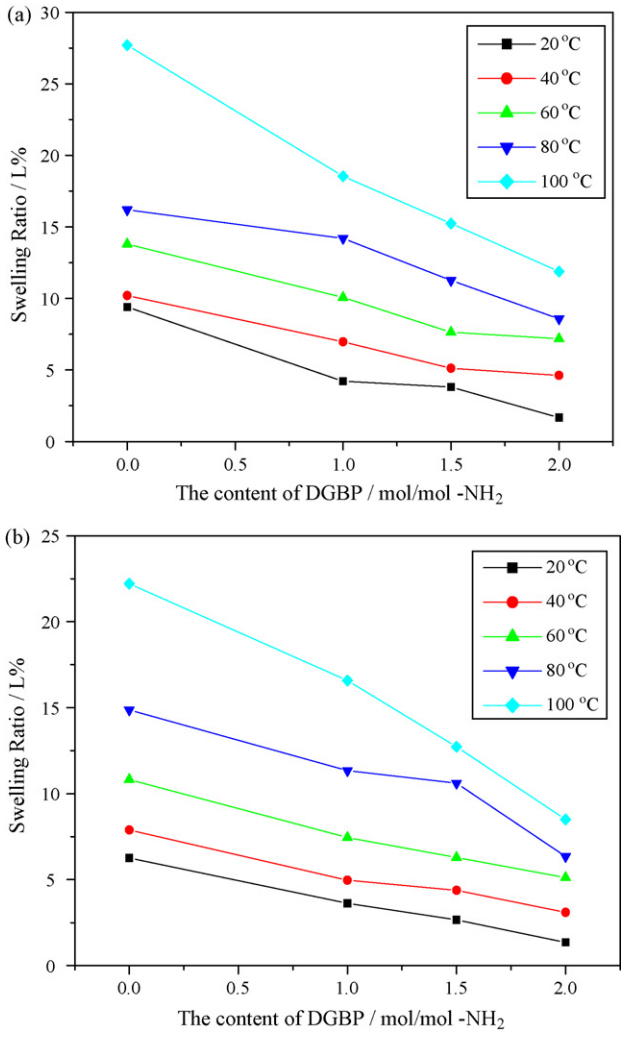

Fig. 8. Swelling ratio of membranes cured at 120 °C (a) and 200 °C (b) with different content of DGBP.

water uptake decrease from 20.2% to 5.6% at room temperature, and from 69.3% to 29.0% at 100 °C. Similarly, the values of swelling ratio decrease from 9.4% to 1.4% at room temperature, and from 27.7% to 8.5% at 100 °C. Comparing Fig. 7(a) with Fig. 7(b), we can see that the water uptake of the membrane with high temperature curing is lower than that with low temperature curing at the same temperature. Similarly, the swelling ratio displays the same trend (Fig. 8). All the values indicate that epoxy crosslinking reaction could play an important role in avoiding excess swelling and improving dimensional stability. It may attribute to two factors. On the one hand, the content of sulfonic acid groups decreases with increasing DGBP in composite membranes. On the other hand, crosslinked network structure hinders water diffusing into membranes.

Table 7
Swelling ratio of membranes at different temperature.

Polymer	Temperature (°C)					
	20		80		100	
	SR_1 [a]	SR_2 [b]	SR_1 [a]	SR_2 [b]	SR_1 [a]	SR_2 [b]
AP6FSPEEK	9.4	6.3	16.2	14.9	27.7	22.2
AP6FSPEEK/DGBP1	4.2	3.6	14.2	11.3	18.5	16.6
AP6FSPEEK/DGBP1.5	3.8	2.7	11.3	10.6	15.2	12.7
AP6FSPEEK/DGBP2	1.7	1.4	8.6	6.4	11.9	8.5

[a] Swelling ratio (%) of membranes cured at 120 °C.
[b] Swelling ratio (%) of membranes cured at 200 °C.

3.6. Proton conductivity of membranes

The proton conductivities of the membranes are estimated using impedance diagrams, and the results at different temperatures are presented in Fig. 9. The proton conductivity of an electrolyte is generally thermally stimulated, which is similar to water uptake of membranes. As shown in Fig. 9, the conductivities of all the samples increase with increasing temperature and decrease with increasing the content of DGBP. It mainly because the total content of water around sulfonic acid groups decreases with increasing DGBP and it is more difficult to move for water molecule in crosslinked network. Thus, the efficiency of proton transmission with water might decrease with increasing DGBP. However, the lowest value of them is still much higher than 10^{-2} S cm^{-1} at room temperature, which is the lowest value for practical interest for usage as PEMs in fuel cells. For example, the proton conductivities of membranes cured at 120 °C are ranged from 9.42×10^{-2} S cm^{-1} to 11.7×10^{-2} S cm^{-1} at 100 °C, which is close to Nafion 117 [41]. Even for the sample of AP6FSPEEK/DGBP1 cured at 200 °C can reach 10.2×10^{-2} S cm^{-1} at 100 °C. The values of AP6FSPEEK/DGBP1 cured at 200 °C at each temperature are close to pure AP6FSPEEK. Comparing with Nafion 117 [46], the value of swelling ratio of AP6FSPEEK/DGBP1 cured at

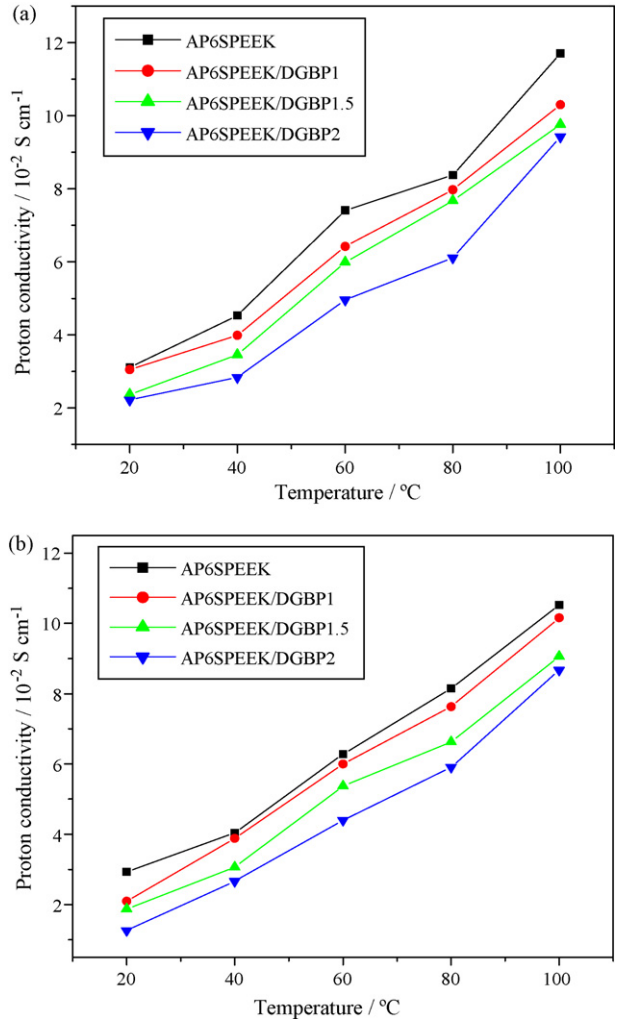

Fig. 9. Proton conductivity of AP6SPEEK and composite membranes cured at 120 °C (a) and 200 °C (b) at different temperatures.

200 °C is much lower. Meanwhile, its conductivity is close to Nafion 117. Considering the water uptake, thermal and dimensional stability, methanol permeability and conductivity, the membrane of AP6FSPEEK/DGBP1 cured at 200 °C might be promising candidate for PEMs.

4. Conclusion

In order to decrease the excessive water uptake and swelling ratio, we provide a simple direct in situ crosslinking method in this work. A series of composite membranes based on AP6FSPEEK and DGBP are cured at two different temperatures. The curing kinetics and application for PEMFCs of composite membranes are investigated. The data show that the crosslinking component effectively improved the properties of the composite membranes. The water uptake of composite membranes cured at 120 °C decreases evidently from 20.2% to 10.1% at room temperature, and from 69.3% to 33.7% at 100 °C, respectively. Whereas after curing at 200 °C, the composite membranes decrease more evidently from 11.6% to 5.6% at room temperature, and 43.6% to 29% at 100 °C, respectively. Meanwhile, the proton conductivities of the samples after curing at 200 °C, are above 5.91×10^{-2} S cm^{-1} and 8.67×10^{-2} S cm^{-1} at 80 °C and 100 °C, respectively. And they all have low methanol permeability with the minimum of 0.33×10^{-6} cm^2 s^{-1} of AP6FSPEEK/DGBP1 cured at 200 °C. All the results exhibited that these crosslinked composite membranes could be promising membranes for fuel cell applications.

References

[1] M.A. Hickner, H. Ghassemi, Y.S. Kim, B.R. Einsla, J.E. McGrath, Chem. Rev. 104 (2004) 4587–4612.
[2] J. Roziere, D.J. Jones, Annu. Rev. Mater. Res. 33 (2003) 503–555.
[3] B.J. Liu, G.P. Robertson, M.D. Guiver, Z.Q. Shi, T. Navessin, S. Holdcroft, Macromol. Rapid Commun. 27 (2006) 1411–1417.
[4] B.J. Liu, G.P. Robertson, D.S. Kim, M.D. Guiver, W. Hu, Z. Jiang, Macromolecules 40 (2007) 1934–1944.
[5] J.A. Kerres, J. Membr. Sci. 185 (2001) 3–27.
[6] Y. Yang, S. Holdcroft, Fuel Cells 5 (2005) 171–186.
[7] R. Nolte, K. Ledjeff, M. Bauer, R. Mulhaupt, J. Membr. Sci. 83 (1993) 211–220.
[8] K. Miyatake, H. Zhou, M. Watanabe, Macromolecules 37 (2004) 4956–4960.
[9] H.B. Zhang, J.H. Pang, D. Wang, A.Z. Li, X.F. Li, Z. Jiang, J. Membr. Sci. 264 (2005) 56–64.
[10] D.J. Jones, J. Rozière, J. Membr. Sci. 185 (2001) 41–58.
[11] B.J. Liu, W. Hu, C.H. Chen, Z.H. Jiang, W.J. Zhang, Z.W. Wu, T. Matsumoto, Polymer 45 (2004) 3241–3247.
[12] P.X. Xing, G.P. Robertson, M.D. Guiver, S.D. Mikhailenko, S. Kaliaguine, J. Polym. Sci. Pt. A: Polym. Chem. 42 (2004) 2866–2876.
[13] P.X. Xing, G.P. Robertson, M.D. Guiver, S.D. Mikhailenko, S. Kaliaguine, Macromolecules 37 (2004) 7960–7967.
[14] A. Roy, H.S. Lee, J.E. McGrath, Polymer 49 (2008) 5037–5044.
[15] B.J. Liu, W. Hu, G.P. Robertson, M.D. Guiver, J. Mater. Chem. 18 (2008) 4675–4682.
[16] C.H. Lee, H.B. Park, Y.S. Chung, Y.M. Lee, B.D. Freeman, Macromolecules 39 (2006) 755–764.
[17] S.L. Zhong, X.J. Cui, H.L. Cai, T.Z. Fu, C. Zhao, H. Na, J. Power Sources 164 (2007) 65–72.
[18] J. Gu, S.C. Narang, E.M. Pearce, J. Appl. Polym. Sci. 30 (1985) 2997–3007.
[19] R.J. Norgan, E.T. Mones, W.J. Steele, Polymer 23 (1982) 295–305.
[20] J.Y. Lee, M.J. Shim, S.W. Kim, Mater. Chem. Phys. 48 (1997) 36–40.
[21] Y.F. Duann, T.M. Liu, K.C. Cheng, W.F. Su, Polym. Degrad. Stab. 84 (2004) 305–310.
[22] J.K.H. Teo, K.C. Teo, B.H. Pan, Y. Xiao, X.H. Lu, Polymer 48 (2007) 5671–5680.
[23] Y.L. Liu, Y.J. Chen, W.L. Wei, Polymer 44 (2003) 6465–6473.
[24] K. Mimura, H. Ito, Polymer 43 (2002) 7559–7566.
[25] W.F.A. Su, J. Polym. Sci. Pt. A: Polym. Chem. 31 (1993) 3251–3256.
[26] W.F.A. Su, K.F.S. JR, J.D.B. Smith, J. Appl. Polym. Sci. 70 (1998) 2163–2167.
[27] W.F. Su, H.W. Huang, W.P. Pan, Thermochim. Acta 392/393 (2002) 391–394.
[28] T.Z. Fu, C.J. Zhao, S.L. Zhong, G. Zhang, K. Shao, H.Q. Zhang, J. Wang, H. Na, J. Power Sources 165 (2007) 708–716.
[29] M.M. Guo, B.J. Liu, Z. Liu, L.F. Wang, Z.H. Jiang, J. Power Sources 189 (2009) 894–901.
[30] B.J. Liu, Y. Dai, G.P. Robertson, M.D. Guiver, W. Hu, Z.H. Jiang, Polymer 46 (2005) 11279–11287.
[31] F. Wang, T.L. Chen, J.P. Xu, Macromol. Chem. Phys. 199 (1998) 1421–1426.
[32] C.L. Zhang, H. Na, C.G. Liu, Z.Y. Ge, Thermosetting Resin 17 (2002) 1–3.
[33] Z. Dai, Y.F. Li, S.G. Yang, C.Z. Zong, X.K. Lu, J. Xu, J. Appl. Polym. Sci. 106 (2007) 1476–1481.
[34] W.B. Liu, Q.H. Qiu, J. Wang, Z.C. Huo, H. Sun, Polymer 49 (2008) 4399–4405.
[35] J. Rocks, L. Rintoul, F. Vohwinkel, G. George, Polymer 45 (2004) 6799–6811.
[36] X. Ramis, J.M. Salla, C. Mas, A. Mantecón, A. Serra, J. Appl. Polym. Sci. 92 (2004) 381–393.
[37] V.L. Zvetkov, Polymer 42 (2001) 6687–6697.
[38] H.E. Kissinger, Anal. Chem. 29 (1957) 1702–1706.
[39] T. Ozawa, Bull. Chem. Soc. Jpn. 38 (1965) 1881–1886.
[40] L.W. Crane, P.J. Dynes, D.H. Kaelble, J. Polym. Sci.: Polym. Lett. Ed. 11 (1973) 533–540.
[41] J. Pang, H. Zhang, X. Li, Z. Jiang, Macromolecules 40 (2007) 9435–9442.
[42] J. Pang, H. Zhang, X. Li, B. Liu, Z. Jiang, J. Power Sources 184 (2008) 1–8.
[43] M. Gil, X. Ji, X. Li, H. Na, J.E. Hampsey, Y. Lu, J. Membr. Sci. 234 (2004) 75–81.
[44] L. Li, J. Zhang, Y.X. Wang, J. Membr. Sci. 226 (2003) 159–167.
[45] T.A. Zawodzinski, J. Davey, J. Valerio, S. Gottesfeld, Electrochim. Acta 40 (1995) 297–302.
[46] J. Pang, H. Zhang, X. Li, D. Ren, Z. Jiang, Macromol. Rapid Commun. 28 (2007) 2332–2338.